ISSN 1330-3651 (Print), ISSN 1848-6339 (Online) https://doi.org/10.17559/TV-20230922000953
Original scientific paper

Ensemble Empirical Mode Decomposition for Automated Denoising of Pulse Signals

Zhiyuan LI*, Mingju YAO

Abstract: Pulse signals are often corrupted by noise, compromising signal integrity for downstream analysis. This paper presents an automated denoising technique for pulse waveforms using ensemble empirical mode decomposition (EEMD). The EEMD algorithm decomposes the signal into intrinsic mode functions (IMFs). Statistical metrics of IMF energy and entropy identify noise components for targeted removal via nonlinear filtering. Experiments on simulated pulse echoes demonstrated the approach of accurately eliminated noise regions. Compared to wavelet decomposition and Monte Carlo methods, the EEMD technique exhibited superior noise reduction and over 90% faster processing. This ensemble empirical mode decomposition approach provides an efficient, data-driven methodology for denoising pulse waveforms with applications in biomedical signal analysis.

Keywords: ensemble empirical mode decomposition; kurtosis detection; ranking entropy; signal denoising; weak laser pulse signal

1 INTRODUCTION

In the field of 3D imaging, data point sets are generated through scanning technologies that target specific objects. However, these scanning methods are subject to various influencing factors that can degrade the quality of the data acquired. During the detection phase, weak pulse signals are particularly vulnerable to multiple forms of interference [1, 2]. Common sources of such interference include circuit noise, atmospheric disturbances, and stray light, all of which contribute to noise within the weak pulse signal. This noise, in turn, compromises the ultimate quality of the 3D imaging output. Consequently, enhancing the quality of 3D imaging necessitates the removal of this signal noise. Against this backdrop, there are exploring methods for the denoising of weak pulse [3, 4].

Signals hold significant practical importance. By examining the relationship between the wavelet decomposition coefficient and the wavelet basis, one can derive the cross-correlation between the original pulse signal and the wavelet decomposition coefficient [5, 6]. This analysis facilitates the selection of an appropriate decomposition level and wavelet basis, thereby enabling signal denoising. However, this approach falls short in effectively isolating the noise components within weak pulse signals and suffers from limited accuracy in noise detection. Another prevalent technique involves extracting multi-dimensional spatio-temporal correlations from the pulse echo signals through matching analysis [7]. This is followed by a two-dimensional transformation of these signals during a hard threshold shrinkage process. Denoising is then completed via a weighted aggregation method [8, 9]. However, this approach still leaves residual weak signals in the denoised output, leading to suboptimal denoising efficacy. Alternatively, one could employ a hybrid method that merges the variational mode decomposition algorithm with the genetic algorithm, guided by the mutual informtion criterion. In this setup, the entropy of the noisy signal serves as the fitness function for the genetic algorithm. This allows for the optimization of parameters within the variational mode decomposition algorithm, facilitating more effective signal denoising [10]. Despite its potential for accuracy, this method suffers from a significant drawback - its time-consuming nature leads to low denoising efficiency.

Existing methods struggle to accurately detect and differentiate noise from desired signal components in laser pulse signals. This can lead to incomplete denoising, resulting in residual noise even after denoising. Additionally, certain denoising techniques may not effectively remove all types of noise present in laser pulse signals. For instance, they may have poor performance in reducing circuit noise, atmospheric interference, or stray light, leading to noise artifacts in the denoised signal [11, 12].

The ensemble empirical mode decomposition (EMD) method used in this study can effectively detect noise in weak laser pulse signals and efficiently denoise the detected noise signals.

2 LITERATURE REVIEW

Automatic noise detection techniques have been widely applied in audio processing, image processing, and signal processing. Based on methods such as machine learning, digital signal processing, and statistical models, automatic noise detection and classification can be performed on input signals. By utilizing automatic noise detection, the accuracy and efficiency of signal processing can be improved, providing a better foundation for subsequent signal processing tasks (Jane, 2021). However, determining the threshold for automatic noise techniques can be challenging.

In recent years, methods based on Empirical Mode Decomposition (EMD) have garnered considerable attention within the field of signal processing [13]. This technique decomposes a signal into a series of Intrinsic Mode Functions (IMFs), which capture the local characteristics of the original data across varying time scales (Ryan, 2000). Distinct from Fourier and wavelet decompositions, EMD is inherently adaptive and does not necessitate predefined basis functions. This versatility makes it broadly applicable across a range of data processing scenarios.

2.1 Laser Pulse Signal Acquisition

In cutting-edge sectors, technologies like lasers and laser electronics have become ubiquitous, finding

applications in laser communication, distance ranging, target identification, and early warning systems (Wang, 2022). Serving as the cornerstone of laser technology, laser pulse signals are instrumental not only in detection and transmission tasks but also in gauging the overall efficacy of various laser technology applications. The quality of laser pulse signal acquisition, encompassing both noise levels and accuracy, has a direct bearing on the effectiveness of its applications. Traditional methods of acquiring these signals frequently introduce high levels of internal noise, as well as distortions or attenuations during transmission, compromising the accuracy of the laser pulse signals (Taken, 202). To mitigate these challenges, there is a pressing need for research into optimized methods for laser pulse signal acquisition, aimed at enhancing the precision of the signals obtained.

2.2 Empirical Mode Decomposition

Empirical Mode Decomposition (EMD) is an adaptive data decomposition technique that relies on the intrinsic properties of the signal in question [14]. This approach can deconstruct complex data from any domain into a finite set of Intrinsic Mode Function components (IMFs). These IMFs adeptly capture the local characteristics of the original data across various time scales (Ryan, 2000). Diverging from Fourier and wavelet decompositions, EMD's adaptability allows its basis functions to be derived directly from the data, eliminating the need for predefined functions. This inherent flexibility has made EMD a widely utilized tool in the realm of data processing.

2.3 Ensemble Empirical Mode Decomposition

While Empirical Mode Decomposition (EMD) is generally effective, it may not fully decompose local feature components across multiple time scales. In cases involving signals with sudden shifts in time scales, mode mixing frequently occurs during decomposition [15]. This compromises the accuracy with which the Intrinsic Mode Function components (IMFs) capture the intrinsic modes of the original signal, thereby diminishing the method's applicability and predictive reliability (Morita, 2018). Ensemble Empirical Mode Decomposition (EEMD) addresses these shortcomings by introducing Gaussian white noise into the original signal. Since this noise has a zero mean, it is effectively nullified through successive averaging computations. This process allows for the automatic allocation of the signal across suitable time scales, and the final ensemble mean serves as the representative calculated result. EEMD follows the following steps [16]:

(1) Gaussian white noise is introduced into the initial signal to enhance the decomposition process. Typically, the ratio (q) of the noise amplitude to that of the original signal is selected within a range of 0.1 to 0.4.

(2) Execute Empirical Mode Decomposition (EMD) on the signal augmented with white noise to yield a collection of Intrinsic Mode Function (IMF) components.

(3) Repeat steps 1 and 2, introducing fresh white noise in each iteration, for a total of (N) repetitions. In this study, (N) is set at 200, as empirical evidence suggests that decomposition performance improves when (N) is a multiple of 100.

(4) Compute the mean of each Intrinsic Mode Function (IMF) component to arrive at the final decomposition outcome.

In light of this literature review, it is evident that automatic denoising methods for weak laser pulse signals, grounded in Empirical Mode Decomposition, offer substantial promise within the domain of signal processing. Nonetheless, there remain challenges and avenues for refinement, particularly in the aspects of algorithmic efficiency and stability [17].

3 RESEARCH METHODS

To address the challenge of denoising weak laser signals, this article employs the following research methodology.

(1) Data Acquisition: Utilize suitable measurement techniques and equipment to collect weak laser pulse signal data.

(2) Empirical Mode Decomposition (EMD): Implement the EMD algorithm to break down the acquired signal into a series of Intrinsic Mode Functions (IMFs). EMD serves as an adaptive, data-driven approach that effectively partitions the signal into its oscillatory components.

(3) Noise Identification: Conduct a thorough analysis of the Intrinsic Mode Functions (IMFs) to isolate components indicative of noise. This identification can be accomplished by scrutinizing the frequency content, amplitude characteristics, or statistical properties of each IMF.

(4) Denoising Technique: Employ denoising methodologies on the isolated noise components within the IMFs. A variety of techniques may be utilized, ranging from thresholding and filtering to adaptive signal processing algorithms.

(5) Reconstruction: Reassemble the denoised signal by amalgamating the processed Intrinsic Mode Functions (IMFs) with those IMFs that encapsulate the desired signal components.

(6) Performance Evaluation: Assess the efficacy of the denoising methodology using suitable metrics, which may include the signal-to-noise ratio (SNR), mean square error (MSE), or visual inspection techniques.

(7) Validation and Optimization: Confirm the efficacy of the denoising approach by juxtaposing the denoised signal against reference signals or ground-truth data. If required, fine-tune the denoising parameters or algorithms to enhance performance.

(8) Experimental Validation: Implement the denoising methodology on actual weak laser pulse signal data and evaluate its performance within real-world applications.

Table 1 Parameter setting of simulation signal dataset

Parameter	Setting
Duration of each sample signal	1 s
Sampling rate	33200 Hz
Pulse signal Type	{CW, LFM, HFM}
Pulse signal bandwidth	500-4000 Hz
Pulse signl center Frequency	{Gaussian noise, stable distribution noise}
Signl-to-noise	–10-10 dB

The signl dataset used in this article is shown in Tab. 1.

The EMD used in this article avoids issues like mode mixing that occur in EMD by adding noise and performing multiple repeated decompositions. This approach also overcomes the inefficiency and low accuracy problems of traditional noise filtering techniques.

4 EXPERIMENT AND RESULTS

4.1 Simulation of Weak Pulse Signal

A model for weak pulse signals is developed, typically comprising components such as random noise, smoke backscattering echoes, and target echo signals. The mathematical expression for this model is as follows:

$$G(t) = r(t) + h(t) + d(t) \tag{1}$$

In its operational state, the transmitter generally emits a bell-shaped wave signal. The mathematical expression representing this weak pulse signal waveform is as follows:

$$w(t) = \exp[-\frac{(T-T_0)^2}{2\upsilon^2}] \tag{2}$$

In this expression, the pulse width corresponding to the waveform and the time at which the peak waveform occurs are specified. It has been observed that the power of the transmitted signal, after undergoing energy attenuation, substantially impacts the characteristics of the echo impulse response:

$$h(t) = \frac{w(t)4\sqrt{\pi}A_r(c)}{\upsilon} \tag{3}$$

Here, the energy attenuation power of the target echo is denoted, and its calculation is defined as follows:

$$A_r(c) = \frac{A - 2cZ_{\max}}{\pi Z} \tag{4}$$

In the given equation, one term represents the detection length of the detector, while another term denotes the peak power of the pulse signal. Additional parameters are influenced by the smoke environment and correspond to the attenuation coefficient associated with the energy of the transmitted signal. Another term signifies the system's overall transmittance during operation, and yet another pertains to the detector's corresponding aperture area. Lastly, a term is designated for the smoke density [18].

The pulse echo signal, as captured by the detector in an ideal environment, is expressed as follows:

$$d(t) = w(t) \otimes h(t) \tag{5}$$

Here, the term signifies the convolution operation. The energy accumulation during the propagation process is modeled using scalar radiation transport theory. One variable represents the corresponding scattering cross-section of soot particles, while another denotes the absorption cross-section of such particles in the air. The light intensity rate undergoes attenuation due to the combined effects of particle scattering and absorption, with the attenuation quantified by a subsequent formula:

$$dO(\vec{r},\hat{s}) = -\rho ds(\varsigma_a + \varsigma_s)O(\vec{r},\hat{s}) \tag{6}$$

In this context, one term serves as the unit vector, another refers to the extinction cross-section associated with the soot particle, and yet another indicates the rate of light intensity incident on a unit volume element. Finally, a term is used to denote the position vector located within the volume element.

4.2 Ensemble Empirical Mode Decomposition of Weak Pulse Signal

In applying the Ensemble Empirical Mode Decomposition (EEMD) technique to dissect weak pulse signals, Gaussian white noise is infused into the residual components. The method calculates the average value of paired components to mitigate false elements and diminish the extent of mode mixing. This study employs the EEMD approach to break down the weak pulse signal in the following manner:

(1) Utilizing the Empirical Mode Decomposition (EMD) technique, we perform a secondary expansion of the weak pulse signal. In this context, one term symbolizes the signal-to-noise ratio, while another represents the zero-mean Gaussian white noise. By calculating the average value of these components, we derive the Intrinsic Mode Function (*IMF*).

$$IMF_1 = \frac{\sum_{i=1}^{m} R_1\left[x(t) + \phi_0 e^i(t)\right]}{m} \tag{7}$$

In the given formula, represents the th empirical mode component derived from the decomposition of the secondary weak pulse signal through the empirical mode decomposition algorithm.

(2) Calculating the residual error magnitude for the weak pulse signal.

(3) Conducting an expansive decomposition and selecting the first mode function acquired through this process as the intrinsic mode function within the empirical mode set:

$$IMF_2(t) = \frac{\sum_{i=1}^{m} R_1\left\{r_1(t) + \phi_1 R_1\left[e^i(t)\right]\right\}}{m} \tag{9}$$

(4) Deriving the th remaining residual quantity of the weak pulse signal using a similar approach:

$$r_k(t) = r_{k-1}(t) - IMF_k(t) \tag{10}$$

(5) In the decomposition process, the first function obtained considered the intrinsic mode function within the set of empirical modes:

$$IMF_{k+1} = \frac{\sum_{i=1}^{m} R_1 \left\{ r_k(t) + \phi_k R_k \left[e^i(t) \right] \right\}}{m} \tag{11}$$

And (6) In the decomposition process, if the weak pulse signal lacks an extreme point or has only one, then the decomposition is considered complete. However, if the weak pulse signal has multiple extreme points, the algorithm reverts to step (4) to finalize the residual error quantity associated with the weak pulse signals. This residual error quantity serves as an indicator of the number of modes. The reconstructed weak pulse signals can be represented as follows:

$$r_{\text{end}}(t) = x(t) - \sum_{L-1}^{L} IMF_k \tag{12}$$

4.3 Rank Entropy of Modal Components

In this study, we outline the methodology for processing weak pulse signal time series through the application of ranking entropy, as follows: Reconstruct the time series of the weak pulse signal to acquire a new series, where the parameters for time delay and embedding dimension are duly represented. Subsequently, sort the elements within this sequence to derive the ordered series.

$$X(t) = \left\{ x(t), x(t+\mu), \cdots, x\left[t + \mu(q-1) \right] \right\} \tag{13}$$

Within the multidimensional space, various mapped symbol sequences emerge. In this study, the ordering entropy of modal components is characterized following the framework of Shannon entropy. The elimination of spurious components is determined based on the resulting calculations.

$$J_A = -\sum_{i=1}^{l} \left(A_i \ln A_i \right) \tag{14}$$

Within the given formula, it represents the probability of the occurrence of symbol sequences of a particular type within the space. The sorting entropy attains its peak value in the given scenario. Consequently, this paper employs the subsequent formula to normalize the sorting entropy.

Through an examination of the provided formula, it becomes evident that sorting entropy serves as a metric for gauging the intricacy and stochastic nature of nonlinear data sequences. As the data sequence's regularity diminishes, the sorting entropy tends to increase.

4.4 Determination of Noise Region of Weak Pulse Signal Based on Kurtosis Test

The approach employed here involves a windowing method rooted in kurtosis testing to identify the noise component within the weak pulse signal. The precise detection procedure is outlined as follows:

(1) Equally divide the time domain according to the specified length to generate segments, ensuring that the length is kept as small as possible to enhance resolution.

(2) Establishing an initial threshold value and performing initialization processing.

(3) Calculating the kurtosis of the weak pulse signal.

(4) In this scenario, it signifies that the signal originating from the noise region has now transitioned into the segment containing pertinent useful signal information. The serial number of the sampling point at this juncture is duly recorded. Conversely, when this point indicates the absence of a distinct boundary between the noise signal and the useful signal, proceed to the subsequent step.

(5) Assessing the presence of boundary points within the weak pulse signal. If no such point is identified, extract the preceding section sequence from the signal. Conversely, if the initial boundary point of the weak pulse signal emerges within this section, merge the noise region to create a new signal.

(6) Reiterate the procedure until reaching the conclusion, ceasing the iteration upon reaching the trailing end of the weak pulse signal, and partitioning a noise region within the weak pulse signal.

4.5 Signal Denoising

Within the noise region, the weak pulse signal undergoes denoising processing via the fusion of the Ensemble Empirical Mode Decomposition method and sorting entropy. The detailed procedure is outlined as follows:

(1) Decompose a weak pulse signal using the ensemble empirical mode decomposition method to yield multiple components;

(2) Sort the components in ascending order of frequency, thereby excluding erroneous elements, and subsequently compute the sorting entropy of the weak pulse signal components;

(3) Rearrange the weak pulse signal components based on the magnitude of their ordering entropy, followed by the implementation of a wavelet filter to perform denoising on the weak pulse signals:

Consider a weak pulse signal containing noise, represented as follows:

$$x = \begin{bmatrix} x_1 \\ x_2 \\ \vdots \\ x_{m+1} \end{bmatrix} = \begin{pmatrix} r_{11} & 0 & \cdots & r_{1n} \\ 0 & r_{22} & \cdots & r_{2n} \\ & \vdots & & \\ 0 & 0 & \cdots & r_{nn} \end{pmatrix} \begin{bmatrix} z_1 \\ z_2 \\ \vdots \\ c \end{bmatrix} = Rz \tag{15}$$

Let denote the noise component of a weak pulse signal. Let be an N-dimensional vector containing the original weak pulse signals. The observed signal can be modeled as: where is a mixing matrix and is a noise vector. The goal is to recover the original signals from the observed noisy mixed signals.

The coefficient matrix and independent components are determined using a wavelet filter, resulting in independent components corresponding to the noise within the weak pulse signal. By eliminating these noise-independent components, a denoised weak pulse signal is derived, expressed as follows:

$$y=\left(y_1,...,y_{n-1},y_c\right)^T$$
$$y'=\left(y_1,...,y_{n-1},0\right)^T \quad (16)$$
$$x'=W^{-1}y'$$

Based on the aforementioned steps, the automatic denoising of the weak pulse signal is successfully accomplished.

5 DISCUSSION

To ascertain the comprehensive effectiveness of the proposed automated denoising method for pulse signals, a simulation experiment is conducted. The pulse energy parameters are set as shown in Tab. 2.

Table 2 Pulse energy parameters

Parameter	Specification
Pulse frequency	55 Hz
Peak power	6.5 kW
Pulse energy	9 J/cm^2
Pulse width	10 ns

Against this backdrop, a model for weak pulse signals is constructed to simulate the characteristics of such signals, as depicted in Fig. 1.

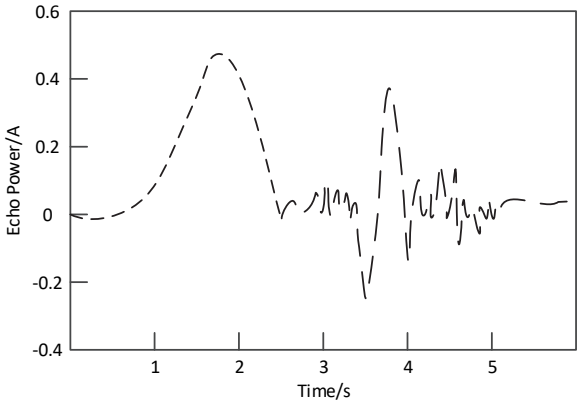

Figure 1 Simulation diagram of weak pulse signal

As evident from Fig. 1, this study effectively simulates the signal echo, resulting in the acquisition of the pulse echo signal. The approach outlined in this paper is employed to segment the noise region within the weak pulse signal, with the resulting divisions illustrated in Fig. 2.

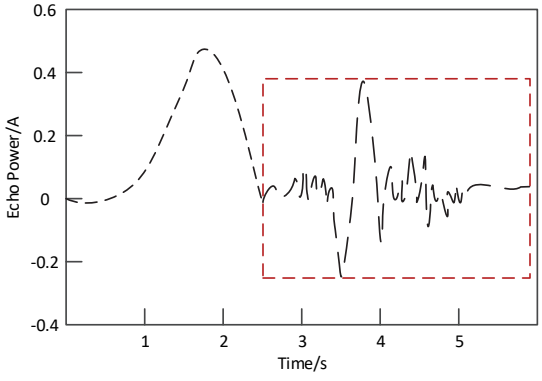

Figure 2 Noise region division result

Denoising tests on the weak pulse signal are conducted, with the method from reference [19], the approach from reference [20], and the method detailed in [21] serving as the comparative methods. The weak pulse signal containing noise is depicted in Fig. 3.

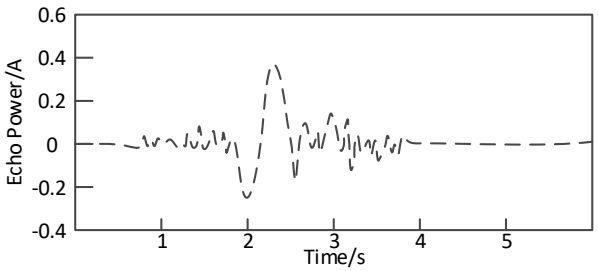

Figure 3 Noisy weak pulse signal

Initially, the proposed method, along with the wavelet decomposition method, the genetic algorithm noise decomposition method, and the semi-analytical Monte Carlo method, is employed to identify the noise region within the weak pulse signal. The outcomes of this detection are presented in Fig. 4.

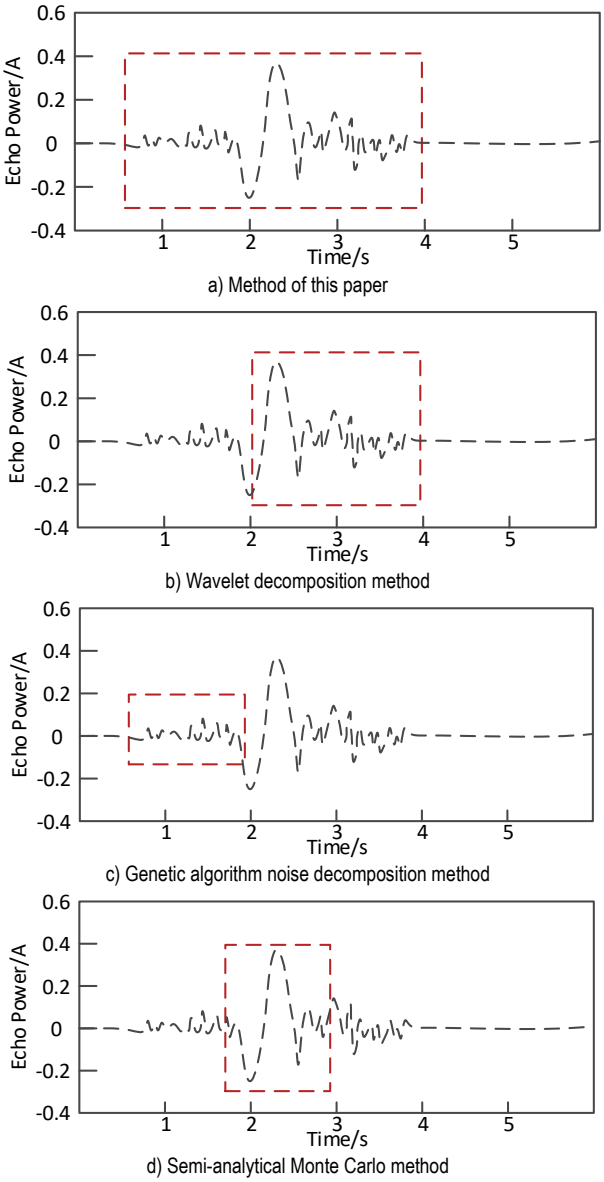

Figure 4 Noise region detection results of different methods

Fig. 4 clearly demonstrates that only the proposed method effectively detects the entire noise region within the weak pulse signal. In contrast, the remaining three methods exhibit incomplete detection of the noise region, managing to identify only a portion of the noise. The aforementioned approach is utilized to perform denoising processing on weak pulse signals, with the outcomes displayed in Fig. 5.

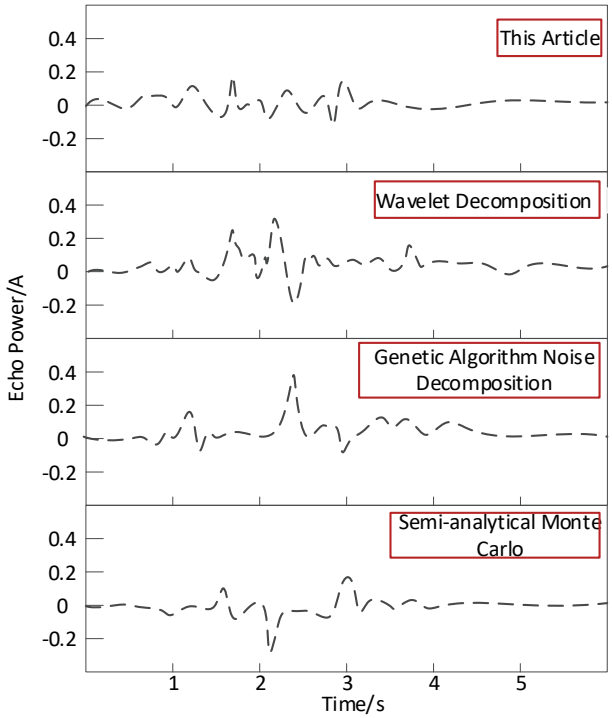

Figure 5 Denoising effect of different methods

Observing Fig. 5, it becomes apparent that in contrast to the original weak pulse signal containing noise, all four methods - namely, the proposed method, the wavelet decomposition method, the genetic algorithm noise decomposition method, and the semi-analytical Monte Carlo method - manage to decrease signal fluctuations. However, upon a comparative assessment of denoising outcomes, the proposed method stands out for its notably pronounced and superior denoising effect. To evaluate the denoising efficiency of the aforementioned methods, we employ the orthogonality index (IO) and denoising time as testing metrics.

Table 3 Denoising efficiency of different methods

Method	Denoising time / s	IO
The proposed method	0.256	0.0022
Wavelet decomposition method	0.884	0.0082
Noise decomposition method based on genetic algorithm	0.946	0.0047
Semi-analytical Monte Carlo method	0.746	0.0057

The denoising efficiency of the method increases with lower values for the above two indicators. Upon analyzing the data in Tab. 3, it becomes evident that in the context of denoising weak pulse signals, the proposed method notably outperforms the other three techniques in terms of denoising time. This is attributed to the ability of the proposed method to accurately identify the noise portion within the weak pulse signal before denoising, thereby shortening the denoising duration. In terms of the orthogonality index (IO), the proposed method also exhibits the lowest value. This stems from its utilization of the ensemble empirical mode decomposition method, which effectively mitigates mode aliasing and enhances the signal decomposition efficiency of the approach.

Although the method proposed in this article can effectively detect and remove noise from laser pulse signals in simulation experiments, it still faces some unexpected problems in the implementation of actual biomedical signals, such as inconsistent pulse intensity of the signal and erroneous noise removal. Further in-depth research is needed to address these issues.

6 CONCLUSION

This study introduces an automated denoising method tailored for pulse signals, aiming to overcome limitations in existing techniques characterized by inadequate noise detection, insufficient denoising effectiveness, and sluggish processing. The novel approach leverages the distinctive echo attributes of pulse waveforms to identify segments containing noise within the signal. By amalgamating ensemble empirical mode decomposition with sorting entropy, this method accomplishes rapid and thorough noise reduction. A key innovation is the precise identification of noise components within the signal, enabling targeted and precise filtering. In practical testing, the algorithm consistently eliminated noise from weak pulse signals. In comparison to prevailing methods, it exhibited superior denoising capabilities while preserving signal integrity and achieving high computational efficiency. These advantages have the potential to bolster the reliability of pulse waveform analysis in biomedical applications. Future exploration could assess the technique's applicability to other low-amplitude biosignals. With further refinements in execution speed and noise discrimination, this approach may find widespread use in the domain of biomedical signal processing. EEMD has potential applications and impacts in the analysis of biomedical signals. It can help improve signal quality, extract key features, assist in disease diagnosis and monitoring, and play a significant role in biomedical engineering and research.

In conclusion, the proposed automated denoising technique introduces a novel means to extract clean pulse signals efficiently and robustly.

Acknowledgements

This work was supported in part by the Sichuan Science and Technology Program, China (No. 2023JDR01942021JQ-379).

7 REFERENCES

[1] Ma, F., Liu, Z.-M., & Guo, F. (2019). Direct position determination for wideband sources using fast approximation. *IEEE Transactions on Vehicular Technology*, *68*(8), 8216-8221. https://doi.org/10.1109/TVT.2019.2921981

[2] Ulman, R. & Geraniotis, E. (1999). Wideband TDOA/FDOA processing using summation of short-time CAF's. *IEEE Transactions on Signal Processing*, *47*(12), 3193-3200.

https://doi.org/10.1109/78.806065
[3] Ho, K. C. & Wenwei, X. (2004). An accurate algebraic solution for moving source location using TDOA and FDOA measurements. *IEEE Transactions on Signal Processing*, *52*, 2453-2463. https://doi.org/10.1109/TSP.2004.831921
[4] Moon, T. K. & Stirling, W. C. (2000). *Mathematical Methods and Algorithms for Signal Processing*. Prentice-Hall, Englewood Cliffs, NJ, USA.
[5] Ma, F., Guo, Z. M., & Guo, F. (2019). Direct position determination in asynchronous sensor networks. *IEEE Transactions on Vehicular Technology*, *68*(9), 8790-8803. https://doi.org/10.1109/TVT.2019.2928638
[6] Naveen, P., Haw, S. C., & Nadthan, D. (2023). Improving chatbot performance using hybrid deep learning approach. *Journal of System and Management Sciences*, *13*(3), 505-516. https://doi.org/10.33168/JSMS.2023.0334
[7] Altarawneh, I. & Albloush, A. (2023). Factors affecting the development of women entrepreneurs: a comprehensive model for Arab countries. *Journal of System and Management Science*s, *13*(3), 381-393. https://doi.org/10.33168/JSMS.2023.0326
[8] Liu., H. & Zhang, T. (2021). Efficient radar detection of weak manoeuvring targets using a coarse-to-fine strategy. *IET Radar, Sonar & Navigation*, *15*(2), 181-193. https://doi.org/10.1049/RSN2.12028
[9] Rajagukguk, S. A., Prabowo, H., Bandur, A., & Setiowati, R. (2023). Behind the rank: the synthesis of a causal model of variables influencing times higher education university ranking. *Journal of System and Management Sciences*, *13*(3), 364-380. https://doi.org/10.33168/JSMS.2023.0325
[10] Wessel, N., Riedl, M., & Kurths, J. (2019). Is the normal heart rate "chaotic" due to respiration. *Chaos*, *19*(2), 028508. https://doi.org/10.1063/1.3133128
[11] Ibrahim, J. & Gajin, S. (2022). Entropy-based Network Traffic Anomaly Classification Method Resilient to Deception. *Computer Science and Information Systems*, *19*(1), 87-116. https://doi.org/10.2298/CSIS2012290451
[12] Yu, S., Lu, J., & Chen, G. (2007). Theoretical design and circuit implementation of multidirectional multi-torus chaotic attractors. *IEEE Transactions on Circuits and Systems I: Regular Papers*, *54*(9), 2087-2098. https://doi.org/10.1109/TCSI.2007.904651
[13] Chen, T., Li, M., Li, Y., Lin, M., Wang, N., & Wang, M. (2015). A Flexible and Efficient Machine Learning Library for Heterogeneous Distributed Systems. *Computer Science*, 1512, 01274. https://doi.org/10.4850/arxiv.1512.01274
[14] Huynh, C. B. D., Nguyen, A. H., Nguyen, T. H. T., & Le, A. H. (2023). Factors affecting students' intention to use mobile learning at universities: an empirical study. *Journal of System and Management Sciences*, *13*(1), 281-304. https://doi.org/10.33168/JSMS.2023.0116
[15] Kingma, D. P., & Adam, J. (2014). A Method for Stochastic Optimization. *arXivpreprint*, *1412*, 6980. https://doi.org/10.48550/arxiv.1412.6980
[16] Wenbo, W., Xiaodong, Z., & Xiangli, W. (2013). Chaotic signal denoising method based on independent component analysis and empirical mode decomposition. *Acta Physica Sinica, 5*(50), 201-050201. https://doi.org/10.7498/APS.62.050201
[17] Gorbunova, M., Masek, P., Komarov, M., & Ometov, M. (2022). A Distributed Ledger Technology: State-of-the-Art and Current Challenges. *Computer Science and Information Systems*, *19*(1), 65-85. https://doi.org/10.2298/CSIS210215037G
[18] Lv, D., Cao, W., Hu, W., & Wu, M. (2021). A new total variation denoising algorithm for piecewise constant signals based on nonconvex penalty. *Neural Computing for Advanced Applications*, *1449*, 633-644. https://doi.org/10.1007/978-981-16-5188-5_45
[19] Nayak, S., Panigrahi., C. R., & Pati, B. (2022). Comparative Analysis of HAR Datasets Using Classification Algorithms. *Computer Science and Information Systems*, *19*(1), 47-63. https://doi.org/10.2298/CSIS201221043N=
[20] Chambolle, A., Duval, V., Peyre´, G, & Poon, C. (2016). Geometric properties of solutions to the total variation denoisingproblem. *Inverse Problems*, *34*(1), 015002. https://doi.org/10.1088/0266-5611/33/1/015002
[21] Iglesias, J. A., Mercier, G., & Scherzer, O. (2018). A note on convergence of solutions of total variation regularized linear inverse problems. *Inverse Problems*, *34*(5), 055011. https://doi.org/10.1088/1361-6420/AAB92A

Contact information:

Zhiyuan LI, Associate Professor
(Corresponding author)
School of Intelligence Technology,
Geely University of China, Chengdu,
Sichuan, 641423, P. R. China
No. 123, SEC. 2, Chengjian Avenue, Eastern New District,
Chengdu City, Sichuan Province
E-mail: lizhiyuan@guc.edu.cn

Mingju YAO, Master Lecturer
School of Intelligence Technology,
Geely University of China, Chengdu,
Sichuan, 641423, P. R. China
No. 123, SEC. 2, Chengjian Avenue, Eastern New District,
Chengdu City, Sichuan Province
E-mail: yaomingju@guc.edu.cn